LETTERS

Optically controlled locking of the nuclear field via coherent dark-state spectroscopy

Xiaodong Xu[1]*, Wang Yao[4]*, Bo Sun[1]*, Duncan G. Steel[1], Allan S. Bracker[2], Daniel Gammon[2] & L. J. Sham[3]

A single electron or hole spin trapped inside a semiconductor quantum dot forms the foundation for many proposed quantum logic devices[1–6]. In group III–V materials, the resonance and coherence between two ground states of the single spin are inevitably affected by the lattice nuclear spins through the hyperfine interaction[7–9], while the dynamics of the single spin also influence the nuclear environment[10–15]. Recent efforts[12,16] have been made to protect the coherence of spins in quantum dots by suppressing the nuclear spin fluctuations. However, coherent control of a single spin in a single dot with simultaneous suppression of the nuclear fluctuations has yet to be achieved. Here we report the suppression of nuclear field fluctuations in a singly charged quantum dot to well below the thermal value, as shown by an enhancement of the single electron spin dephasing time T_2*, which we measure using coherent dark-state spectroscopy. The suppression of nuclear fluctuations is found to result from a hole-spin assisted dynamic nuclear spin polarization feedback process, where the stable value of the nuclear field is determined only by the laser frequencies at fixed laser powers. This nuclear field locking is further demonstrated in a three-laser measurement, indicating a possible enhancement of the electron spin T_2* by a factor of several hundred. This is a simple and powerful method of enhancing the electron spin coherence time without use of 'spin echo'-type techniques[8,12]. We expect that our results will enable the reproducible preparation of the nuclear spin environment for repetitive control and measurement of a single spin with minimal statistical broadening.

We performed the experiment on a single negatively charged quantum dot embedded in a Schottky diode structure. Figure 1a shows the four-level energy diagram of the trion states under an external magnetic field perpendicular to the sample growth direction. In the pump–probe experiment, two narrow-linewidth continuous wave lasers selectively excite a three-level lambda subsystem, as shown in the dashed box of Fig. 1a (ref. 17; see Methods Summary). When the pump and probe lasers exactly match the two-photon Raman resonance (TPR) condition, a coherent superposition of the spin ground states are formed[18]. This is known as the dark state[19] and represents a coherent manipulation of the electron spin in the frequency domain (a brief comparison of ref. 18 with the

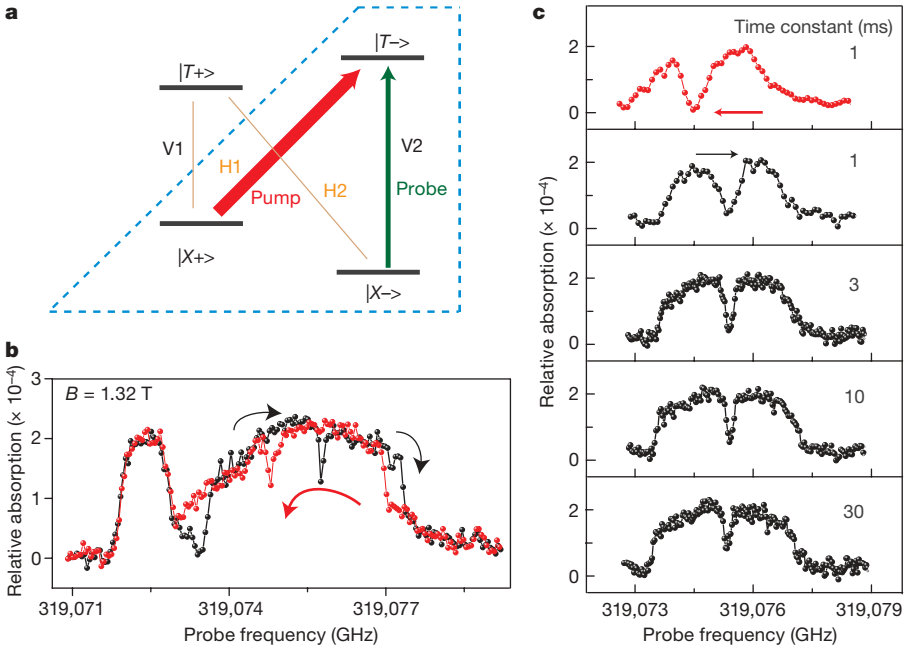

Figure 1 | Laser frequency sweep direction dependent probe absorption spectrum. a, The trion energy level diagram with a magnetic field applied in the Voigt geometry. The blue dashed box indicates the selected three-level Lambda system. A strong pump beam is near-resonant with transition H1 and a weak beam probes transition V2. **b**, The probe absorption spectrum at an external magnetic field of 1.32 T. The black (or red) curve represents the probe absorption spectrum of the forward (or backward) scan. **c**, The probe absorption spectrum as a function of the laser scan rate, indicated by the lock-in time constant. The top red curve is the backward scan with a 1-ms lock-in time constant.

[1]The H. M. Randall Laboratory of Physics, The University of Michigan, Ann Arbor, Michigan 48109, USA. [2]Naval Research Laboratory, Washington DC 20375, USA. [3]Department of Physics, University of California San Diego, La Jolla, California 92093, USA. [4]Department of Physics, The University of Hong Kong, Hong Kong, China.
*These authors contributed equally to this work.

current experiment can be found in the Supplementary Information). Because absorption of the probe laser by trion excitation increases abruptly with detuning from the TPR, the generated dark state is very sensitive to small changes in the nuclear field, which can affect the TPR and hence can be used as an *in situ* probe of the nuclear spin environment in a quantum dot[20].

Figure 1b shows the probe absorption spectrum at a magnetic field of 1.32 T. The black curve is the spectrum obtained by sweeping the probe laser from low frequency to high frequency (the forward scan). The red curve is the spectrum obtained by sweeping the probe laser from high frequency to low frequency (the backward scan). The narrow peak on the left and the broad peak on the right correspond to transitions H2 and V2, respectively. We focus on the optical response from transition V2.

Ideally, the overall lineshape of transition V2 should be Lorentzian-like with a dark-state dip, as shown in Fig. 4a. However, the spectrum clearly shows a broadened lineshape with a round top and sharp edges, which is far from Lorentzian. The width and the strength of the dip corresponding to the dark state are also narrower and shallower than expected. More remarkably, we observe hysteresis at the sharp edges of the V2 absorption peak between the forward and backward scans. Additionally, the spectral position of the dark state in each scan is shifted in the same direction as the scan, which indicates a change of TPR when the scan direction is switched. The external magnetic field is unchanged in the forward and backward scans, so these observations indicate that we optically create and probe the dynamic nuclear spin polarization (DNP) in this charged quantum dot system, where the nuclear spin configuration depends on the laser sweeping direction.

The dependence on laser scan rate is shown in Fig. 1c. The dark state becomes more pronounced, concomitant with a broader dip width as we increase the laser scan rate (that is, the probe laser frequency is held for a shorter interval at each value). Under faster scans, the observed lineshape is closer to the standard dark-state spectrum in a Lambda level scheme (compare Fig. 4a). As we show below, the anomalous spectral features and their scan-rate dependence reflect the dynamical control of the nuclear field by the laser frequency scans on a timescale comparable to the nuclear spin relaxation time, which is of the order of a second[12,14,16].

We performed a set of measurements by fixing the frequencies of both lasers and recording the optical response as a function of time; these measurements reveal that the DNP modifies the Zeeman splitting, via the nuclear field, to maximize the trion excitation. Figure 2a shows the probe absorption spectra with forward (black) and backward (red) scans. We begin by scanning the laser backward and stopping the laser just before the sharp rising edge of the trion peak, as shown by the green curve in Fig. 2b. We record the absorption signal as a function of time with the laser frequency fixed. As shown in Fig. 2c, the system remains in hysteresis state 1 for a while (shown by the signal level) and then abruptly switches into hysteresis state 2, where it remains. This signifies that the nuclear field switches to a stable value that maximizes the trion excitation. Finally, we scan the probe laser forward and find that the subsequent partial forward scan spectrum (the blue curve in Fig. 2d) overlaps considerably with its equivalent in the full forward scan.

We also examined the dynamics of the nuclear spin by monitoring the dark state. As shown in Fig. 2e, after a full forward scan to locate the dark-state position (black curve), we took a partial forward scan

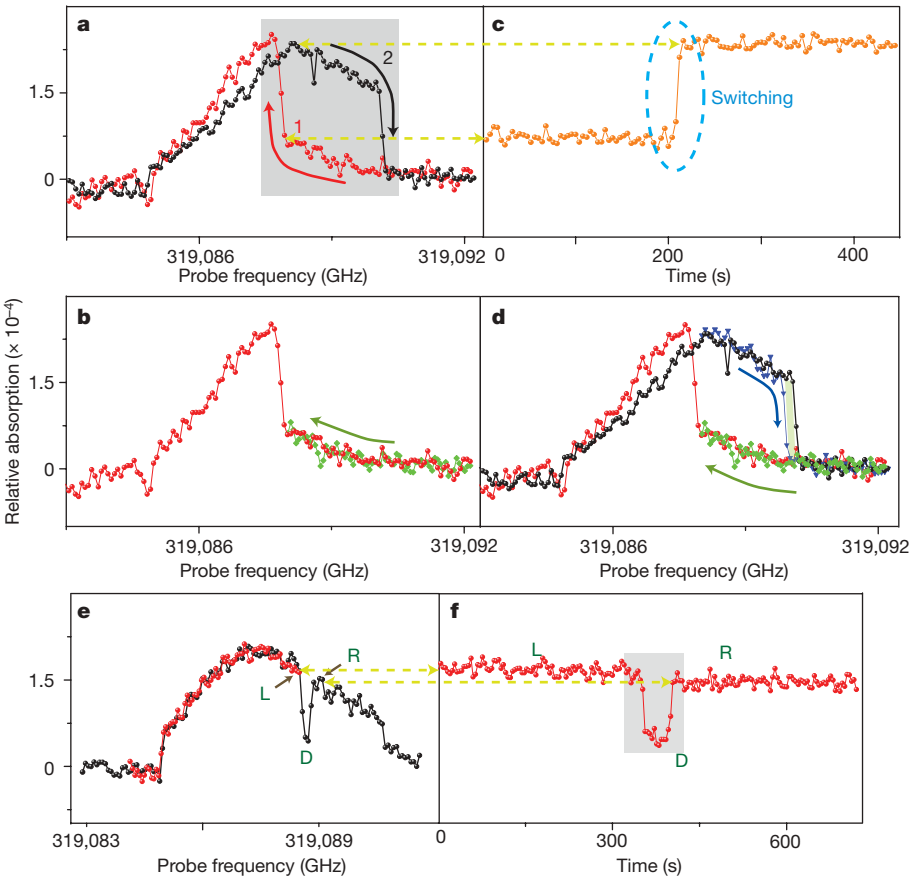

Figure 2 | Time-dependent probe absorption spectrum with fixed laser frequencies. Data are taken at a magnetic field of 2.64 T. **a**, The black (or red) curve represents a full forward (or backward) scan. **b**, The green curve is a partial backward scan. **c**, The probe absorption signal taken as a function of time immediately after stopping the laser just before the rising edge of the trion absorption. **d**, The blue curve is the partial forward scan taken after the switching of the hysteresis states. **e**, The black (or red) curve is the full forward (or partial forward) scan. L, D and R denote three system configurations. **f**, The absorption signal as a function of time, taken immediately after parking the laser just before the dark state is formed.

to prepare the initial nuclear spin configuration and stopped tuning the laser just before the formation of the dark state (red curve). Immediately, we measured the absorption signal as a function of time (Fig. 2f). The system starts in configuration L, indicated by the signal level, jumps into configuration D after some time, and then switches to configuration R, where it remains at high probe absorption. In experiments we noticed that the system can stay in the dark state D on a timescale from a few seconds to 3 min, indicating the meta-stable nature of the nuclear configuration at the TPR (see also the Supplementary Information). Figure 2f shows an example in which the system stays in the D configuration for ~40 s.

Power-dependent measurements of the dark state with a fast laser scan rate provide frequency domain information on the electron spin coherence time. Figure 3a shows the decreasing trend of the estimated spin decoherence rate $\gamma_s/2\pi$ with the increase of the square root of the pump intensities. The black dots represent $\gamma_s/2\pi$ inferred from the absorption minimum at the dark-state dip (normalized by the absorption maximum at the trion peak) and the blue triangles are values extracted from the best fit of the dark-state spectrum including the DNP dynamics. An example of the dark-state spectrum is given in Fig. 3b (identical to Supplementary Fig. S1 with pump Rabi of 0.9 GHz). Details of the data analysis leading to Fig. 3a can be found in the first section of Supplementary Information. For this time-ensemble-averaged measurement of a single spin, γ_s^{-1} corresponds to the inhomogeneous dephasing time T_2* because of the measurement-to-measurement fluctuations of the nuclear field. For our dot, we estimate the spin inhomogeneous broadening due to a thermally distributed nuclear environment to be (360 ± 30) MHz (refs 7, 21). The dark-state spectrum clearly shows that the spin T_2* has been enhanced well above the thermal value. As we show later, the enhancement of electron spin T_2* is a natural result from the suppression of nuclear spin fluctuations by the positive DNP feedback process and the data in Fig. 3a is a lower bound of this enhancement effect. This mechanism is in fact far more powerful in enhancing the spin T_2* than the preliminary results from Fig. 3a and b suggest, as we will show using a different experimental set-up.

Both the rounded and broadened trion peak in the probe spectrum and the switching behaviours at fixed laser frequencies indicate that large trion excitation is favoured by the DNP process. When a trion is excited, its two constituent electron spins form an inert singlet, leaving its hole constituent to interact with the nuclear spins. This is a unique element for optical control of the nuclear spin environment while manipulating the electron spin, and it accounts for the experimental observations here.

The hyperfine interaction between the hole spin and nuclear spin is strongly anisotropic[22,23]. In particular, it has a non-collinear hyperfine coupling term $S_h^X I_k^Z$, where S_h^X is the heavy-hole pseudospin operator along the field direction (**X**) and I_k^Z is the nuclear spin operator along the growth direction (**Z**). This interaction can flip a nuclear spin without flipping the hole spin, costing only the nuclear Zeeman energy: $\hbar\omega_N \approx 0.01\,\mathrm{GHz\,T^{-1}}$ (refs 24 and 25). This process stands out from the various DNP interactions because the small energy cost can be directly compensated by the homogeneous broadening of the trion state (~0.4 GHz), which is a lower-order process than the electron-nuclear flipflops assisted by phonons or photons.

From Fermi's Golden Rule, the nuclear spin flip rates are proportional to $\rho_{t,i}\rho_{t,f}$, where $\rho_{t,i}$ is the initial-state trion population and $\rho_{t,f}$ is the final-state trion population after a nuclear spin flip (see details in Supplementary Information). This is because $S_h^X I_k^Z$ has non-zero matrix elements only in the trion portion of the steady-state wave function. The up and down nuclear spin flip rates are different, because they change the electron Zeeman splitting—and hence the two-photon detuning δ from the TPR—in opposite ways, each of which lead to different final-state trion populations $\rho_{t,f}$. Clearly, the

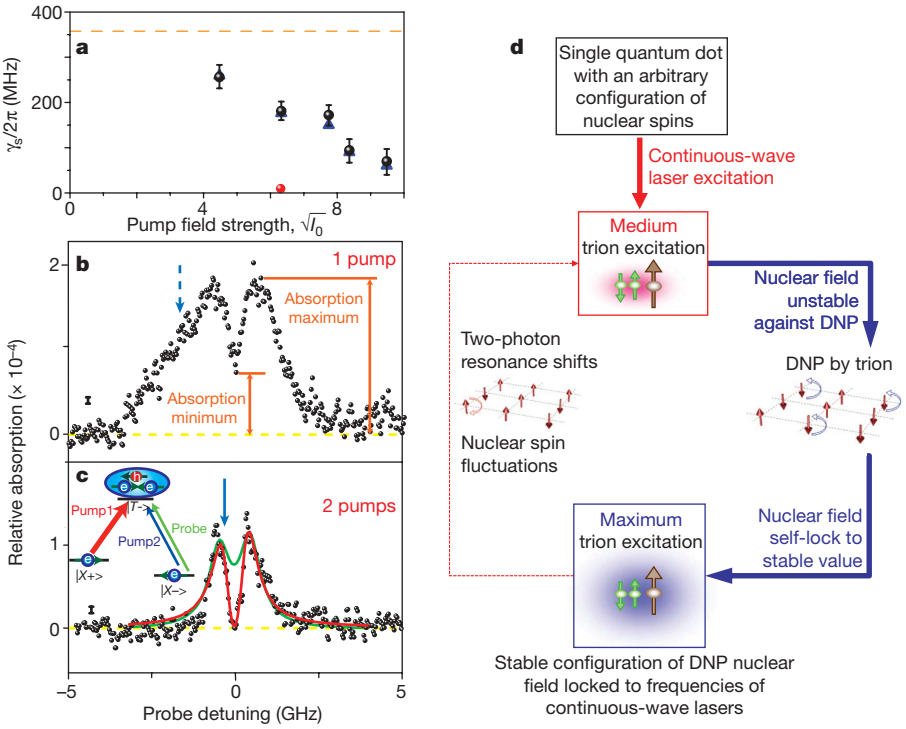

Figure 3 | The observation of the enhancement of electron spin T_2*. **a**, The estimated $\gamma_s/2\pi$ from the two-beam dark-state spectrum with various pump field strengths, where $I_o = 2\,\mathrm{W\,cm^{-2}}$. Black dots and blue triangles are estimated from the dip-to-peak absorption ratio with error bars determined from the measurement noise (see black error bar symbol in **b**) and from the best fits of the spectrum by modelling the nuclear field dynamics (see Supplementary Information), respectively. The dashed horizontal line denotes the thermal value. The red dot is from fitting the three-beam spectrum in **c**. **b**, An example of the dark-state spectra obtained by fast forward scan in the two-beam set-up that yields the $\gamma_s/2\pi$ value in **a**. The yellow dashed line denotes the zero signal line. **c**, A three-beam measurement with the schematic set-up shown in the inset. The solid blue arrow indicates the spectral position of the second pump beam (also indicated in **b** as a reference with the dashed blue arrow). **d**, Schematic illustration of the self-locking DNP feedback process, which locks the nuclear field to a stable value that maximizes trion excitation.

one resulting in a larger $\rho_{t,f}$ always 'wins', that is, the DNP process tends to maximize trion excitation. The net DNP rate is proportional to $\rho_t(\partial\rho_t/\partial\delta)$, which goes to zero at the maxima of the trion excitation (also the position of strongest absorption), located at $\delta = \pm\Omega_{pump}/2$, where Ω_{pump} is the pump Rabi frequency (see Fig. 4b). The DNP process functions as a restoring force around the absorption maxima, such that when the laser is slightly detuned from the position of the strongest trion excitation, DNP acts to adjust the Zeeman splitting to maximize the trion excitation. We note that the net DNP rate is also zero at the TPR because it is a local minimum, which ties in with the meta-stable nature of the dark state observed in Fig. 2f.

We numerically simulate the self-locking process by including DNP into the optical Bloch equations (see Supplementary Information). Figure 4c simulates the result for fast scans, and Fig. 4d for slow scans, at magnetic field 1.32 T. The numerical simulations qualitatively reproduce the important features of the experimental observations. Figure 4e clearly shows that the resulting nuclear fields differ greatly depending on whether the probe frequency is scanned forward or backward, which explains the origins of the edge hysteresis and the spectral shift of the dark state. We note that the asymmetry between the forward and backward scans in Fig. 2a is due to the pump detuning (see Supplementary Fig. S3a).

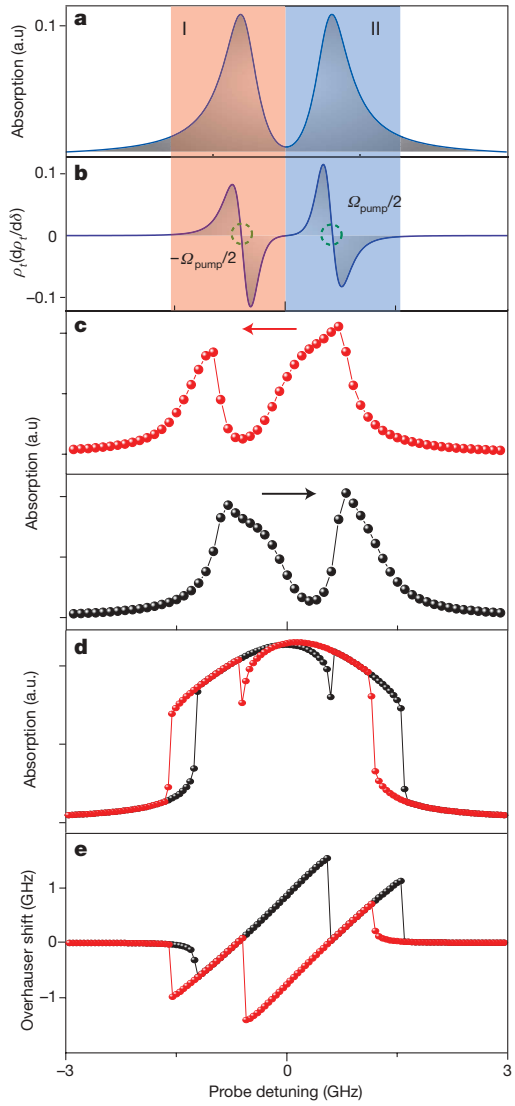

Figure 4 | Theoretical explanation of the nuclear field self-locking effect through the DNP feedback process. **a**, **b**, The calculated probe absorption spectrum (**a**) and $\rho_t(\partial\rho_t/\partial\delta)$ (**b**) by solving the three-level Lambda system with pump on resonance in the absence of DNP. **b** shows the DNP acting as a restoring force. The two stability regions corresponding to the absorption maxima are labelled I and II. **c**, **d**, Numerical simulation results including the self-locking DNP effects for fast (**c**) and slow (**d**) scan corresponding to a magnetic field of 1.32 T. The black (or red) curve represents the probe absorption spectrum of the forward (or backward) scan. **e**, The calculated nuclear field corresponding to the slow scan. The positive (or negative) nuclear field shifts the probe absorption spectrum to the blue (or red). a.u., arbitrary units.

The self-locking effect described in the theory also leads to the suppression of the nuclear spin fluctuations. Once the system has switched to a configuration of maximum trion excitation, the electron spin Zeeman energy and hence the nuclear field are determined and controlled only by the instantaneous laser frequencies, regardless of the initial nuclear spin configuration before the scan starts. In this regime, DNP can actively work to maximize the trion population, and any nuclear spin fluctuations that shift the Zeeman resonance are cancelled out through feedback via the DNP mechanism (Fig. 3d). The quantitative enhancement of T_2* by this mechanism is determined by the slope of the DNP rate as a function of detuning at the locking points, that is, the two circled positions in Fig. 4b at $\pm\Omega_{pump}/2$. A larger slope means a stronger restoring force, and hence a better locking effect (see Supplementary Fig. S3b, which is qualitatively consistent with the trend shown in Fig. 3a). For spectra discussed in Fig. 3a and b, the locking position of the nuclear field follows the probe laser, which scans much faster than the DNP equilibration rate, so the suppression effect we obtained there is a lower bound of the capability of this nuclear field-locking technique.

Consequently, if the pump and probe beams are fixed spectrally to maximize the trion excitation, the nuclear field fluctuations should be suppressed further than when the probe continuously scans, as in Fig. 3b. Data taken using three beams (Fig. 3c) support this argument. The stronger pump 1 remains near-resonant with transition H1 and the weaker pump 2 is tuned to transition V2 and fixed at the spectral position that maximizes the trion absorption. The two pumps lock the nuclear field to a constant value and suppress nuclear fluctuations for the duration of the experiment. We use the weak probe beam to generate the dark-state spectrum with a fast scan rate, shown in Fig. 3c. The probe is weak and scans at a fast rate, so the effect of the probe beam on the nuclear field can be ignored.

The resulting spectrum in Fig. 3c shows a cleaner dark-state lineshape with a more pronounced dip than the two-beam dark-state spectrum in Fig. 3b with comparable pump intensity, which confirms that the nuclear field is locked by the two pumps. The dip strength represents the electron spin T_2* and the measured absorption at the TPR approaches zero, so the data indicate a substantial enhancement of the T_2* in this two-pump set-up. It is challenging to extract an accurate spin decoherence rate because the suppression of nuclear spin fluctuations is so strong that the signal approaches zero at the TPR. However, fitting the data with the standard two-beam optical Bloch equation, the red curve on top of the data (fitting parameters $\Omega_{pump}/2\pi = 0.9$ GHz, $\gamma_t/2\pi = 0.4$ GHz and $\delta_{pump} = -30$ MHz), yields a value for $\gamma_s/2\pi$ of the order of ~1 MHz with a 5 MHz upper bound error bar, limited by the mutual coherence bandwidth between the lasers. We can also estimate the T_2* directly from the absorption minimum at the dark-state dip, although this will not be as accurate as the optical Bloch equation curve fitting because it does not exploit all the data points. This dip-to-peak ratio estimation gives a $\gamma_s/2\pi$ of 2 MHz, which agrees with the optical Bloch equation fit. The green curve on top of the data is a theoretical plot using the thermal value of T_2*, which clearly shows the strong enhancement of the electron spin T_2* by the DNP self-locking effect. The strongly suppressed γ_s indicates that the intrinsic T_2 could possibly be recovered by this nuclear field-locking technique. We expect that a time domain measurement may more accurately show the dramatic enhancement of T_2* by the nuclear field-locking scheme described above. Further measurements and theory to explore this potential are in progress.

In conclusion, our results provide a simple but powerful method of suppressing the nuclear spin fluctuations. Once the nuclear spin environment is prepared by our nuclear field-locking method, it may be possible to perform coherent manipulations of a single electron spin for the entire duration of the intrinsic electron spin coherence time, unaffected by hyperfine-interaction-induced inhomogeneous spin dephasing.

METHODS SUMMARY

We give a brief review of the sample structure and experimental techniques, which are explained in detail in refs 26 and 27. The sample contains InAs self-assembled quantum dots grown by molecular beam epitaxy. The size of the dot is about 3 nm in height and 15 nm in base diameter[28]. The sample is embedded in a Schottky diode structure, so we set the DC voltage to charge only one electron into the dot. We use the DC Stark shift modulation absorption technique to achieve a high signal-to-noise ratio[29]. The modulation amplitude is large so that the data correspond directly to absorption. The sample is held in a continuous helium flow magneto cryostat. The magnetic field can be tuned up to 6.6 T. For the quantum dot of interest, the electron in-plane g factor is 0.49 and the hole in-plane g factor is 0.13. The experiment is performed at a temperature of $\sim$5 K.

Two continuous-wave lasers are used in the experiment. As shown in Fig. 1a, a strong pump (red arrow) is horizontally polarized and fixed to be nearly resonant with transition H1 and the weak probe beam (green arrow) is vertically polarized. In the experiment, the estimated pump Rabi frequency ranges from $\sim$0.63 to $\sim$1.35 GHz, and the probe Rabi frequency is fixed at $\sim$0.24 GHz. Since the polarization axis of the quantum dot is rotated about 20° away from the laboratory frame owing to the heavy and light hole mixing[30], the probe beam can pick up both V2 and H2 transitions in a single scan. For the slow scan data shown in the text, the probe laser frequency is held at each value for 4 s and each data point is the integrated signal over the last 1 s of this interval.

Received 30 November 2008; accepted 5 May 2009.

1. Berezovsky, J. *et al.* Picosecond coherent optical manipulation of a single electron spin in a quantum dot. *Science* **320,** 349–352 (2008).
2. Bracker, A. S. *et al.* Optical pumping of the electronic and nuclear spin of single charge-tunable quantum dots. *Phys. Rev. Lett.* **94,** 047402 (2005).
3. Gammon, D. & Steel, D. G. Optical studies of single quantum dots. *Phys. Today* **55,** 36–41 (2002).
4. Gerardot, B. D. *et al.* Optical pumping of a single hole spin in a quantum dot. *Nature* **451,** 441–444 (2008).
5. Kim, D. *et al.* and nondestructive measurement in a quantum dot molecule. *Phys. Rev. Lett.* **101,** 236804 (2008).
6. Kroutvar, M. *et al.* Optically programmable electron spin memory using semiconductor quantum dots. *Nature* **432,** 81–84 (2004).
7. Merkulov, I. A. Efros, A. L. & Rosen, M. Electron spin relaxation by nuclei in semiconductor quantum dots. *Phys. Rev. B* **65,** 205309 (2002).
8. Petta, J. R. *et al.* Coherent manipulation of coupled electron spins in semiconductor quantum dots. *Science* **309,** 2180–2184 (2005).
9. Baugh, J. Kitamura, Y. Ono, K. & Tarucha, S. Large nuclear Overhauser fields detected in vertically coupled double quantum dots. *Phys. Rev. Lett.* **99,** 096804 (2007).
10. Tartakovskii, A. I. *et al.* Nuclear spin switch in semiconductor quantum dots. *Phys. Rev. Lett.* **98,** 026806 (2007).
11. Eble, B. *et al.* Dynamic nuclear polarization of a single charge-tunable InAs/GaAs quantum dot. *Phys. Rev. B* **74,** 081306 (2006).
12. Greilich, A. *et al.* Nuclei-induced frequency focusing of electron spin coherence. *Science* **317,** 1896–1899 (2007).
13. Koppens, F. H. L. *et al.* Control and detection of singlet-triplet mixing in a random nuclear field. *Science* **309,** 1346–1350 (2005).
14. Maletinsky, P., Lai, C. W., Badolato, A. & Imamoglu, A. Nonlinear dynamics of quantum dot nuclear spins. *Phys. Rev. B* **75,** 035409 (2007).
15. Vink, I. T. *et al.* Locking electron spins into magnetic resonance by electron-nuclear feedback. Preprint at <http://arxiv.org/abs/0902.2659> (2009).
16. Reilly, D. J. *et al.* Suppressing spin qubit dephasing by nuclear state preparation. *Science* **321,** 817–821 (2008).
17. Xu, X. D. *et al.* Fast spin state initialization in a singly charged InAs-GaAs quantum dot by optical cooling. *Phys. Rev. Lett.* **99,** 097401 (2007).
18. Xu, X. *et al.* Coherent population trapping of an electron spin in a single negatively charged quantum dot. *Nature Phys.* **4,** 692–695 (2008).
19. Harris, S. E. Electromagnetically induced transparency. *Phys. Today* **50,** 36–42 (1997).
20. Stepanenko, D., Burkard, G., Giedke, G. & Imamoglu, A. Enhancement of electron spin coherence by optical preparation of nuclear spins. *Phys. Rev. Lett.* **96,** 136401–136404 (2006).
21. Braun, P. F. *et al.* Direct observation of the electron spin relaxation induced by nuclei in quantum dots. *Phys. Rev. Lett.* **94,** 116601 (2005).
22. Eble, B. *et al.* Hole–nuclear spin interaction in quantum dots. *Phys. Rev. Lett.* **102,** 146601–146604 (2009).
23. Fischer, J. Coish, W. A., Bulaev, D. V. & Loss, D. Spin decoherence of a heavy hole coupled to nuclear spins in a quantum dot. *Phys. Rev. B* **78,** 155329 (2008).
24. Kikkawa, J. M. & Awschalom, D. D. All-optical magnetic resonance in semiconductors. *Science* **287,** 473–476 (2000).
25. Gammon, D. *et al.* Nuclear spectroscopy in single quantum dots: nanoscopic raman scattering and nuclear magnetic resonance. *Science* **277,** 85–88 (1997).
26. Ware, M. E. *et al.* Polarized fine structure in the photoluminescence excitation spectrum of a negatively charged quantum dot. *Phys. Rev. Lett.* **95,** 177403 (2005).
27. Xu, X. *et al.* Coherent optical spectroscopy of a strongly driven quantum dot. *Science* **317,** 929–932 (2007).
28. Scheibner, M. *et al.* Optically mapping the electronic structure of coupled quantum dots. *Nature Phys.* **4,** 291–295 (2008).
29. Alen, B. *et al.* Stark-shift modulation absorption spectroscopy of single quantum dots. *Appl. Phys. Lett.* **83,** 2235–2237 (2003).
30. Koudinov, A. V. & Akimov, I. A. Kusrayev, Yu. G. & Henneberger, F. Optical and magnetic anisotropies of the hole states in Stranski-Krastanov quantum dots. *Phys. Rev. B* **70,** 241305 (2004).

Supplementary Information is linked to the online version of the paper at www.nature.com/nature.

Acknowledgements We thank P. L. McEuen, L.-M. Duan, and D. Kim for discussions. This work is supported by US ARO, AFOSR, ONR, NSA/LPS, and FOCUS-NSF.

Author Information Reprints and permissions information is available at www.nature.com/reprints. Correspondence and requests for materials should be addressed to D.G.S. (dst@umich.edu).